Modes of Star Formation and the Origin of Field Populations
ASP Conference Series, Vol. XXXX, 2001
E. K. Grebel and W. Brandner, eds.

The low-mass IMF – deep star counts in the dSph galaxy Ursa Minor

Sofia Feltzing

Lund Observatory, Box 43, SE-221 00 Lund, Sweden

Rosemary Wyse and Mark Houdashelt

Physics & Astronomy Department, Johns Hopkins University, Baltimore, MD 21218, U.S.A.

Gerard Gilmore

Institute of Astronomy, Madingley Road, CB3 0HA Cambridge, U.K.

Abstract. We present a new study of deep star counts in the Local Group dwarf spheroidal (dSph) in Ursa Minor. Both the luminosity function (LF) and the colour-magnitude diagram (CMD) of the unevolved stars are compared with the LF and CMD of the old, metal-poor globular cluster M92. The main sequence locations and turn-offs are identical within the errors. Since we know from the brighter evolved stars that the metallicities for these two disparate systems are the same this implies that they also have equal ages. A direct comparison of faint LFs is then equivalent to comparison of the low-mass stellar Initial Mass Functions (IMF). We find that their LFs are identical within the mass-range covered ($\sim 0.35 - 0.8\ M_{\odot}$). The Ursa Minor dSph has one of the highest apparent M/L ratios known in the Local Group, and is an extremely low surface brightness external galaxy. M92 is a typical high surface brightness globular cluster, with no apparent dark matter. These results lead to the conclusion that the low-mass stellar IMF in systems that formed at high redshift is independent of environment. Indeed, it is consistent with the low-mass IMF in star-forming regions today.

1. Introduction

In the Local Group of galaxies some 20 dwarf spheroidal galaxies (dSph) have been identified (Mateo, 1998). They are some of the most uninteresting objects, to the eye, in the sky with their low surface brightness (around 25 magnitudes per square arcsec in V) spread over a large angle (up to 160 arcmin for Sextans). Yet, they may hold answers to the quest to understand the nature of dark matter. As reviewed recently by Mateo (1998) Local Group dSph galaxies have some of the largest known M/L ratios for a single galaxy, and an order of magnitude larger than that derived for normal spiral galaxies. These large M/L ratios have been inferred from the observed velocity dispersion in the central parts of

these dSph galaxies and are all in excess of the value expected for purely stellar systems with a standard IMF.

The questions then naturally arise of how do these high M/L ratios arise, are they due to truly high dark matter contents or are there other explanations possible? Several alternative suggestions have been put forward; e.g. "artificially" inflated velocity dispersions by tidal effects and projection effects (e.g. Klessen & Kroupa 1998) or by unresolved binary stars, though a very non-standard binary population is required (Hargreaves et al. 1996). True dark matter in these small systems must be cold, but standard non-baryonic CDM provides for dark haloes that are too centrally-concentrated (e.g. Moore 1999). Baryonic dark matter remains a possibility, and here we will investigate whether or not the apparent dark matter simply can be in the form of low-mass stellar objects. The method we have chosen for our investigation is simple; obtain a deep luminosity function of a dSph with lots of apparent dark matter and compare that to the luminosity function of a system known to contain no dark matter, such as a globular cluster.

The dSph chosen should have as narrow as possible ranges of age and metallicity as a mixture of several ages and metallicities would make the experiment more complicated and parameter dependent. Further, we want the dSph to have large amounts of apparent dark matter and the Ursa Minor and Draco dSphs are the two outstanding examples with $(M/L)_0 = 60$ and 58 $(M_\odot/L_\odot)$ as measured in the V-band, respectively (Mateo, 1998, Table 4). Detailed spectroscopic abundance analysis has been done for a few stars in both Draco and Ursa Minor (Stetson 1984 and Shetrone et al. 1998, 2001). The Ursa Minor dSph has, within the errors, one metallicity, [Fe/H]$= -2.2 \pm 0.2$ dex (Stetson 1984), as compared to Draco which has a clearly detected spread in metallicity of about one dex. Stetson (1984) finds a spread of $= -2.9 <$[Fe/H]< -1.8 and the recent Keck observations by Shetrone et al. (1998, 2001) confirms this result. Furthermore the Ursa Minor dSph has a simple star-formation history (consistent with one single early burst of star formation) and no second parameter problem (see e.g. Mateo, 1998) and a negligible reddening, $E(B-V) \simeq 0.03$ (Zinn, 1981). It is also close, $(m-M) = 19.1 \pm 0.1$ (Olszewski & Aaronson, 1985) which means that it is possible to reach deep down on the main sequence.

2. The data

Observations were obtained using the WFPC2 on board HST during 1997, 1998, and 1999 in the two filters F606W and F814W (HST program GO 7419, PI Wyse). The images were processed through the standard pipeline. The final, drizzled images have total exposure times in F606W of 14600 sec and in F814W of 17200 sec. These data supersede the earlier, partial dataset presented in Feltzing et al. (1999). Photometry was derived from the drizzled images using the IRAF DAOPHOT package. Empirical *psf*s were created individually for each filter and image and the χ and sharpness parameters were used to eliminate e.g. unresolved background galaxies. The *psf*-photometry in this way provided a coordinate list that was then used to derive new *psf* fitted photometry using the scheme described by Cool & King (1996). The corresponding colour-magnitude diagrams were then constructed by cross-correlating the stellar coordinates. A

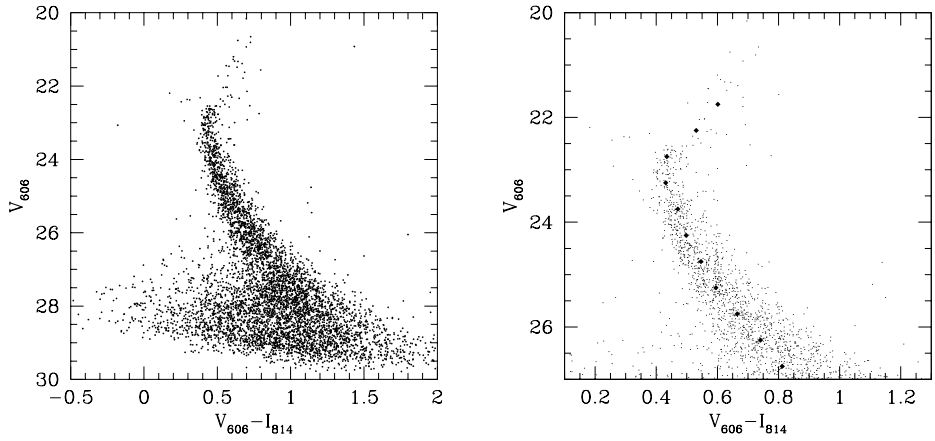

Figure 1. CMD for the Ursa Minor dSph. In the right-hand panel we show a blow-up including a comparison with the fiducial line from the M92 CMD, based on data from Piotto et al. (1997).

total of 2038, 1751, and 1698 stars were detected in this way on WF2, WF3, and WF4, respectively. Completeness has been estimated by adding artificial stars to the drizzled images and then rerunning the detection and photometry procedure described above on the artificial images. The magnitudes for the retrieved artificial stars were compared with their input magnitudes and only stars with input − output = 0.5 magnitudes were kept when completeness was determined.

The luminosity function for each WF was then constructed from the CMDs. The data were, for each WF, then corrected for incompleteness and then all three LFs were combined into one, shown in Fig. 2. The final comparisons between M92 and the Ursa Minor dSph is shown in Fig. 1b (CMD) and 2b (LF). The M92 data have been moved to the same distance modulus as that of the Ursa Minor dSph and renormalized. It is clear from this that down to the 50% completeness limit there is no significant difference between the number of stars at a given magnitude (and thus inferred mass) in the two systems (Fig. 2b). This means that in a system with a high amount of inferred dark matter, Ursa Minor, and in a system with no dark matter, M92, the stellar formation processes are such that the relative numbers of low mass stars are the same. Furthermore, these two systems – a globular cluster and a dSph galaxy – are at opposite extremes of stellar number density, with the central V-band surface brightness of M92 being 15.6 mag/sq arcsec (Harris 1996), while that of the Ursa Minor dSph is 25.5 mag/sq arcsec (Mateo 1998).

As the metallicity of both the Ursa Minor dSph and M92 are known and are very similar we may therefore compare their colour magnitude diagrams to determine whether or not they have differing ages, Fig. 1b. Since the two objects have the same metallicity this plot infers that they have the same age as well. This confirms the recent results by Mighell & Burke (1999).

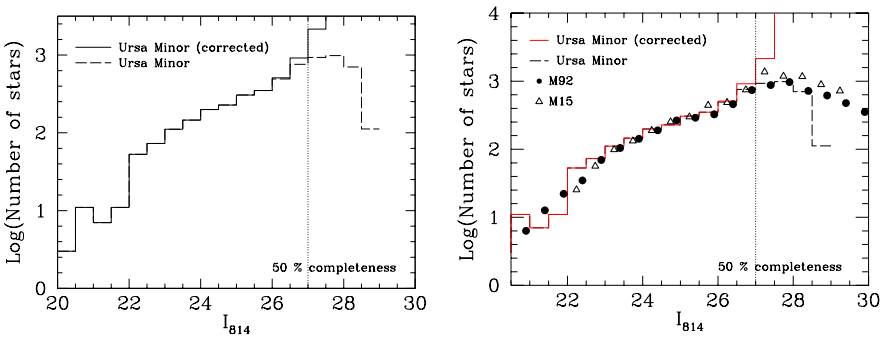

Figure 2. Left panel shows the uncorrected and corrected luminosity function for the Ursa Minor dSph in the I band. The right-hand panel shows the same luminosity functions as well as the LF from the globular cluster M92 as well as that from M15 (Piotto et al. 1997).

3. Binaries

If binary systems are present in a stellar population they may be distinguished in the CMD. The easiest case to detect would arise if all binary systems were made up of two stars with equal mass. In this case the binaries would make up a sequence in the CMD that would have the same colour as the individual stars in the system but $2.5\log(2)$ magnitudes brighter than the main sequence. If the systems are made up of stars of unequal masses there will be a gradual spread of stars between the main sequence and the equal mass sequence Hurley & Tout (1998). Although $V-I$ is not the best discriminatory between single and binary stars (because the main sequence becomes quite vertical in this colour) a spread to the red can clearly be seen in our colour magnitude diagram.

We now proceed to quantify this visual impression. First we determined a fiducial ridge line by binning in V and finding the mean $V-I$ for each bin. This was done using the data for the full CMD for all three chips. Then we selected a clean portion of the main sequence, $24.8 \lesssim V \lesssim 25.8$. In this magnitude range we do not have to concern ourselves with completeness issues. For each star in the selected part of the CMD and for each chip we then calculated the distance to the ridge line. Then we determined the median distance from the ridge line on each chip. Minor differences were found, such that $median(WF4) - median(WF2) = 0.010$ and $median(WF4) - median(WF3) = -0.026$. The median for chip four is -0.016. That the median is negative is to be expected as the fiducial ridge line has constructed using all stars, both binary and single, and is thus redder than the actual main sequence.

A histogram of the distances was then constructed, Fig. 3. The histogram shows a rather typical distribution for a single stellar population with binaries present. It has a fairly steep, Gaussian looking blue side, reaching a flat-ish peak (binaries of unequal mass), then falling off fairly rapidly and showing a tail consisting of equal mass binaries. That these features are correctly interpreted is illustrated by the small histogram for the M92 data that is also shown. M92 is

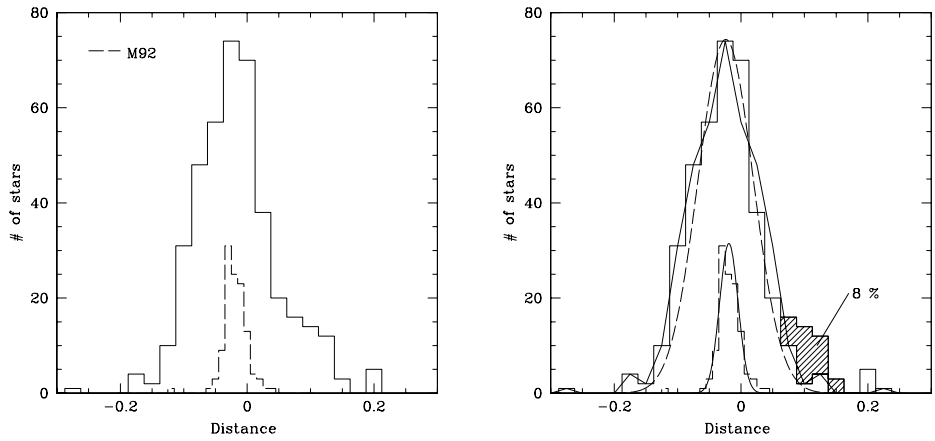

Figure 3. Left panel shows the histogram of the stars perpendicular distances of each stars from the fiducial ridge line of the main sequence for both the Ursa Minor dSph and the globular cluster M92. The right-hand panel shows the same diagrams but also the same Gaussian fitted to the two histograms (full line for M92 and dashed for the Ursa Minor dSph) as well as fit to the blue side of the Ursa Minor histogram that then has been mirrored on to the red side (full line). Finally the binary stars are marked as a shaded area.

known to present at least an 8% binary candidate fraction (Romani & Weinberg, 1991) as derived from ground based CCD photometry.

To estimate the number of equal mass binary systems in the Ursa Minor dSph we simply mirrored the blue part of histogram to the red side and counted the number of stars in the "bump" on the red side, Fig. 3. In this way we find that 8 % of the systems observed are equal mass (or close to equal mass) binaries. These are shown as the shaded area in Fig. 3.

Thus it appears that the Ursa Minor dSph has a normal binary population, indicating that undetected binaries are not the source of the large observed velocity dispersion.

4. The initial mass function in the Ursa Minor dSph

The question to be answered in this study was whether or not the initial mass function (IMF) in the Ursa Minor dSph was different from that in systems so far studied. While our data was not expected to reach to the brown dwarf limit, the indications from the solar neighbourhood (Reid et al. 1999) is that there is a smooth continuity across the M-star – brown dwarf regime, so that should very low mass objects be associated with the dark matter in this dSph, one might expect to see a signal even in the M-dwarf regime to which our data are sensitive. The comparison with M92 shows that there is indeed no excess of low mass stars in the Ursa Minor dSph, down to $\sim 0.35 M_{\odot}$ (using isochrones from Baraffe et al. 1997).

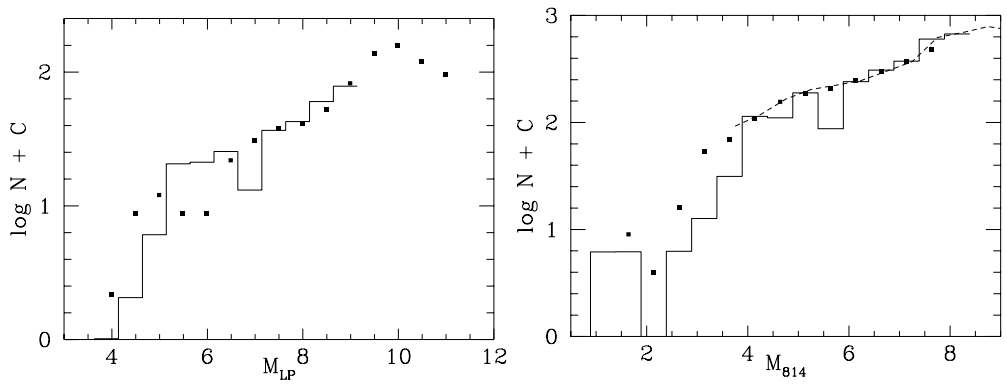

Figure 4. Left panel shows the comparison between the completeness corrected STIS LP LF for the Ursa Minor dSph (solid line) and the globular cluster M15 (filled squares). The right-hand panel shows the a comparison of the STIS-based LF for the Ursa Minor dSph (solid line= with the LF from the WFPC2 data (filled squares). Both are then compared with a theoretical LF that corresponds to a power-law mass function with a slope of −1.35 (dotted line).

We also quantify this by studying our complementary STIS (see Wyse et al. 1999; 2001 in prep.) observations and comparing them to a theoretical mass function, Fig. 4. A mass function of slope −1.35 (where Salpeter is −2.35) is converted into an LF using the Baraffe et al. (1997) models, Fig. 4. The fit to the M92 and hence the Ursa Minor dSph data is good. This is in agreement with what was found for M92 and M15 by Piotto & Zoccali (1999). Further, Zoccali et al. (2000) found this to be an excellent fit to their data for the faint LF of the galactic Bulge, further supporting the universality of the IMF of old stars, across two to three dex in metallicity. This slope is close to that of the solar neighbourhood IMF derived by Scalo (1986), over this mass range.

5. Conclusions

We have done a purely differential study between the faint stellar LF of the Ursa Minor dSph and that of the metal-poor and old globular cluster M92. In summary we find that (a) the luminosity function in the Ursa Minor dSph is the same, at low masses, as that in the globular cluster M92 which leads to the conclusion that the apparent dark matter in the Ursa Minor dSph can not be made up of low mass stars (b) that the Ursa Minor dSph has the same age as globular cluster M92, and (c) that there are binaries present in the Ursa Minor dSph, and that equal mass binaries make up ~ 8 %.

Since this LF and underlying IMF are remarkably similar to that of e.g. the galactic bulge these results intriguingly appear to further indicate the universality of the IMF. In particular it is similar over several dex in metallicity as well as in environments of very different densities, e.g. a tenuous dSph and a dense globular cluster.

Acknowledgement Based on observations with the NASA/ESA Hubble Space Telescope, obtained at STScI, operated by AURA Inc, under NASA contract NAS5-26555. Support for this work was provided by NASA grant number GO-7419 from STScI.

References

Baraffe, I., Chabrier, G., Allard, F, Hauschildt, P., 1997, A&A, 327, 1054

Cool A.M., King I.R., 1996, HST post-calibration workshop, (STScI, Baltimore) p290

Feltzing S., Gilmore G., Wyse R., 1999, ApJ, 516, L17

Hargreaves, J., Gilmore, G., Annan, C. 1996, MNRAS, 279, 108

Harris, W.E., 1996, AJ, 112, 1487

Hurley, J., Tout, C.A., 1998, MNRAS, 300, 977

Klessen, R.S, Kroupa, P., 1998, AJ, 498, 143

Mateo, M., 1998, ARA&A, 36, 435

Mighell, K.J., Burke, C.J., 1999, AJ, 119, 366

Moore, B. Quinn, T., Governato, M., Stadel, T., Lake, G., 1999, MNRAS, 310, 1147

Olszewski, E.W., Aaronson, M., Hill, J.M., 1995, AJ, 110, 2120

Piotto, G., Cool, A., King, I.R., 1997, AJ, 113, 1345

Piotto G., Zoccali M., 1999, A&A, 345, 845

Reid, I.N., et al., 1999, ApJ, 521, 613

Romani, R.W., Weinberg, M.D. 1991, ApJ, 372, 487

Scalo, J.M., 1986, Fund. Cosmic Phys., 11, 1

Shetrone, M., Bolte, M., Stetson, P. 1998, AJ, 115, 1888

Shetrone, M., Cote, P., Sargent, W.L.W., 2001, AJ in press, also astro-ph/0009505

Stetson, P.B., 1984, PASP, 96, 128

Wyse R.F.G., Gilmore G., Feltzing S., Houdashelt M., 1999, in "The Hyredshift Universe: Galaxy Formation and Evolution at High Redshift" ASP Conf.Series 193, eds AJ Bunker and JM van Breugel, p 181

Zinn, R., 1981, ApJ, 251, 52

Zoccali M., Cassisi S., Frogel J., Gould A., et al., 2000, ApJ, 530, 418